OPTICAL FLOW: A CURVE EVOLUTION APPROACH

Arun Kumar, Allen Tannenbaum and Gary Balas

Departments of Aerospace and Electrical Engineering, University of Minnesota
Minneapolis, MN 55455

ABSTRACT

A novel approach for the computation of optical flow based on an L^1 type minimization is presented. It is shown that the approach has inherent advantages since it does not smooth the flow-velocity across the edges and hence preserves edge information. A numerical approach based on computation of evolving curves is proposed for computing the optical flow field and results of experiments are presented.

1. INTRODUCTION

Optical flow field is defined as the velocity vector field of apparent motion of brightness patterns in a sequence of images [5]. In their pioneering work, Horn and Schunk [5] use a quadratic smoothness constraint. The immediate difficulty with this smoothness constraint is that at the object boundaries such a smoothness constraint will have difficulty capturing the optical flow.

In this paper, we propose a novel method for computing optical flow based on the theory of the evolution of curves and surfaces. The approach employs an L^1 type minimization of the norm of the gradient of the optical flow vector. It can be shown that the equations diffuse in a direction orthogonal to the intensity gradients i.e., in a direction along the edges. This results in the edges being preserved. The equations can be solved by following a methodology very similar to the evolution of curves based on the work of Osher and Sethian [11] and Rudin *et al.* [15].

This work was supported in part by grants by the National Science Foundation DMS-8811084, ECS-9122106, by the Air Force Office of Scientific Research AFOSR AF/F49620-94-1-00S8DEF, by the Army Research Office DAAH04-94-G-0054 and DAAH04-93-G-0332, and by Image Evolutions Limited.

2. L^1 MINIMIZATION

Intuitively, it is desired that the "geometry" of the optical flow dictated by the sharp intensity gradients in the images should be captured by the regularization. An L^1 type optimization problem is successful in satisfying this intuition and the solution makes contact with non-linear geometric scale-space ideas.

We use the following L^1 norm smoothing error to develop insights into the optical flow problem:

$$\epsilon_s = \int_\Omega \sqrt{u_x{}^2 + u_y{}^2} + \sqrt{v_x{}^2 + v_y{}^2}\, d\Omega. \quad (2.1)$$

Consider the regularization of the optical flow using the following cost-functional:

$$\min_{(u,v)} \int_\Omega \sqrt{u_x{}^2 + u_y{}^2} + \sqrt{v_x{}^2 + v_y{}^2} + \alpha^2 (E_x u + E_y v + E_t)^2 \, d\Omega.$$

The Euler-Lagrange equations in this case are

$$-\alpha^2 E_x (E_x u + E_y v + E_t) + \frac{\partial}{\partial x}\left(\frac{u_x}{\sqrt{u_x{}^2 + u_y{}^2}}\right) + \frac{\partial}{\partial y}\left(\frac{u_y}{\sqrt{u_x{}^2 + u_y{}^2}}\right) = 0, \quad (2.2)$$

$$-\alpha^2 E_y (E_x u + E_y v + E_t) + \frac{\partial}{\partial x}\left(\frac{v_x}{\sqrt{v_x{}^2 + v_y{}^2}}\right) + \frac{\partial}{\partial y}\left(\frac{v_y}{\sqrt{v_x{}^2 + v_y{}^2}}\right) = 0. \quad (2.3)$$

The "curvature terms" in these equations can be easily identified and the equations rewritten as

$$\kappa_u - \alpha^2 E_x (E_x u + E_y v + E_t) = 0, \quad (2.4)$$

$$\kappa_v - \alpha^2 E_y (E_x u + E_y v + E_t) = 0, \quad (2.5)$$

where the curvatures κ_u and κ_v are given by

$$\kappa_u = \frac{u_x{}^2 u_{yy} - 2u_x u_y u_{xy} + u_y{}^2 u_{xx}}{(u_x{}^2 + u_y{}^2)^{3/2}} = \mathrm{div}\left(\frac{\nabla u}{\|\nabla u\|}\right), \quad (2.6)$$

0-8186-7310-9/95 $4.00 © 1995 IEEE

and

$$\kappa_v = \frac{{v_x}^2 v_{yy} - 2v_x v_y v_{xy} + {v_y}^2 v_{xx}}{({v_x}^2 + {v_y}^2)^{3/2}} = \text{div}\left(\frac{\nabla v}{\|\nabla v\|}\right). \quad (2.7)$$

κ_u and κ_v given in these equations are precisely the curvatures of level sets as we show now; see also [1, 3, 11].

Consider the level set of the differentiable function $\Psi(x, y)$

$$\mathcal{C}_k = \{(x, y) : \Psi(x, y) = k\}, \quad (2.8)$$

where k is a constant. An arc-length parametrization for $\mathcal{C}_k$ is chosen by

$$\mathcal{C}_k = \{(x(s), y(s)) : s \in [0, \mathrm{L}(\mathcal{C}_k)]\}, \quad (2.9)$$

where L(.) denotes the length of the curve. The level set is given as

$$\Psi(x(s), y(s)) = k = \text{constant}. \quad (2.10)$$

Differentiating twice, solving for the various derivatives w.r.t the arc-length and then simply substituting in:

$$\kappa = \frac{x_p y_{pp} - y_p x_{pp}}{(x_p^2 + y_p^2)^{3/2}}. \quad (2.11)$$

we may write the curvature of the implicitly defined curve $\mathcal{C}_k$ as follows:

$$\kappa_\Psi = \frac{\Psi_{xx}\Psi_y^2 - 2\Psi_{xy}\Psi_x\Psi_y + \Psi_{yy}\Psi_x^2}{(\Psi_x^2 + \Psi_y^2)^{3/2}} = \text{div}(\frac{\nabla\Psi}{\|\nabla\Psi\|}). \quad (2.12)$$

We will use gradient descent to solve equations (2.4, 2.5). We introduce a new time (or scale) variable t', and derive the following nonlinear parabolic evolution equations:

$$\hat{u}_{t'} = \kappa_{\hat{u}} - \alpha^2 E_x(E_x\hat{u} + E_y\hat{v} + E_t), \quad (2.13)$$

$$\hat{v}_{t'} = \kappa_{\hat{v}} - \alpha^2 E_y(E_x\hat{u} + E_y\hat{v} + E_t), \quad (2.14)$$

for $\hat{u} = \hat{u}(x, y, t, t')$ and similarly for $\hat{v}$. The steady-state solution of the system (2.13, 2.14) is precisely the solution of the Euler-Lagrange equations (2.4, 2.5). Note that in the limit that $\alpha \longrightarrow 0$, we get the equations:

$$\hat{u}_{t'} = \kappa_{\hat{u}} = \frac{\kappa_{\hat{u}}}{\|\nabla\hat{u}\|}\|\nabla\hat{u}\|, \quad (2.15)$$

$$\hat{v}_{t'} = \kappa_{\hat{v}} = \frac{\kappa_{\hat{v}}}{\|\nabla\hat{v}\|}\|\nabla\hat{v}\|. \quad (2.16)$$

3. NUMERICAL IMPLEMENTATION

A straightforward finite-difference approach to numerically solve for the optical flow from equations (2.13) and (2.14) does not work very well. The two main problems which can arise are the development of singularities and topological changes as the curve evolves. After the singularity develops an entropy condition is imposed on the evolution to pick out the correct solution. The entropy condition employed here is that for a propagating flame: *a particle once burnt remains burnt* and has been used in the work of Osher and Sethian [11] on which our numerical implementation are based.

Osher and Sethian in [11] show that by embedding the curve in a two dimensional surface and then evolving the surface rather than the curve, one derives robust, stable, and reliable evolution algorithms which also incorporate the changes in topology.

We apply the aforementioned numerical methods of Osher and Sethian to the optical flow equations (2.13, 2.14) given in Section 2. α is assumed to be a fixed small positive number and the choice is problem dependent. The numerical algorithm we use is similar to the one developed in Rudin *et al.* [15]. The complete set of discretized equations have been given in [8].

4. RESULTS OF EXPERIMENTS

In this section results are presented for three (two synthetic and one real) sets of images taken from Barron *et al.*, [2].

Sinusoidal sequence

The sinusoidal sequence is a synthetic image sequence and consists of the superposition of two sinusoidal plane-waves Figure 4(a). The correct velocity field has all vectors $\vec{v} = (1, 1)$.

Diverging Tree sequence

This is a synthetic image sequence in which the camera is moved along the line of sight and the focus of expansion is taken as the center of the image, Figure 4(b). The flow field is primarily dilational.

Rotating Rubik Cube Sequence

This sequence shows a Rubik's cube rotating counterclockwise on a turntable see Figure 4(c). The motion field is primarily rotational.

It is observed that the L^1 minimization approach based on curve-evolution is sensitive to intensity gradients and is less diffusive in its computations of the flow fields. For the real image sequence of the Rubik's cube placed on a rotating turntable the flow field computed shows sensitivity to the intensity gradients (due to the local patterns on the turntable's edge and also on the faces of the cube) while at the same time reproducing the global motion of the turntable, see Figure 3(a).

For the synthetic image sequences we have tried to produce the most smooth fields globally by increasing the α parameter. Recall that varying the value of α in the evolution equations gave a scale space with varying degrees of smoothness in the flow field. Larger values of α produces smoother fields while smaller values will capture the edges in the images. Thus for example we are able to capture the divergent field in the diverging tree sequence, see Figures (2), and the translational field in the sinusoidal sequence, see Figures (1).

5. CONCLUSIONS

In this paper we have developed a novel approach for the computation of optical flow from sequence of images. We motivate the use of an L^1–norm minimization of the flow vectors based on the ideas of scale spaces and the geometric heat equation. This approach has inherent advantages since it does not smooth the flow velocity across the edges. The numerical approach to solving the resulting equations is implemented using numerical approaches from the theory of evolution of curves and it has been found to work quite well.

6. REFERENCES

[1] L. Alvarez, F. Guichard P. L. Lions, and J. M. Morel, "Axiomes et equations fondamentales du traitement d'images," *C. R. Acad. Sci. Paris*, 315:135–138, 1992.

[2] J. L. Barron, D. J. Fleet, and S. S. Beauchemin, "Performance of optical flow techniques," *International Journal of Computer Vision*, 12:43–77, 1994.

[3] V. Caselles, F. Catte, T. Coll, and F. Dibos, "A geometric model for active contours in image processing," *AMS*, 29:1–10, 1993.

[4] E. C. Hildreth, "Computations underlying the measurement of visual motion," *Artificial Intelligence*, 23:309–354, 1984.

[5] B. K. P. Horn and B. G. Schunck, "Determining optical flow," *Artificial Intelligence*, 23:185–203, 1981.

[6] B. K. P. Horn, *Robot Vision*, MIT Press, Cambridge, Mass., 1986.

[7] B. B. Kimia, A. Tannenbaum, and S. W. Zucker, "On the evolution of curves via a function of curvature-I: the classical case," *Journal of Math Analysis and Applications*, 163:438–458, 1992.

[8] A. Kumar, A. Tannenbaum, and G. Balas, "Optical Flow: A curve evolution approach," *IEEE Transactions on Image Processing*, submitted.

[9] R. J. LeVeque, *Numerical Method for Conservation Laws*, Birkhauser, 1992.

[10] M. Luettgen, W. C. Karl, and A. Willsky, "Efficient multiscale regularization with applications to the computation of optical flow," *IEEE Trans. Pattern Analysis and Machine Intelligence*, PAMI-3:41–63, 1994.

[11] S. J. Osher and J. A. Sethian, "Fronts propagating with curvature dependent speed: Algorithms based on Hamilton-Jacobi formulations," *Journal of Computational Physics*, 79:12–49, 1988.

[12] P. Perona and J. Malik, "Scale space and edge detection using anisotropic diffusion," *IEEE Trans. Pattern Analysis and Machine Intelligence*, PAMI-12:629–639, 1990.

[13] K. Prazdny, "On the information in optical flows," *Computer Vision, Graphics, and Image Processing*, 23:239–259, 1983.

[14] J. G. Rosen, "The gradient projection method for nonlinear programming, II: nonlinear constraints," *J. Soc. Indust. Appl. Math*, 9:514–532, 1961.

[15] L. I. Rudin, S. Osher, and E. Fatemi, "Nonlinear total variation based noise removal algorithms," *Physica D*, 60:259–268, 1993.

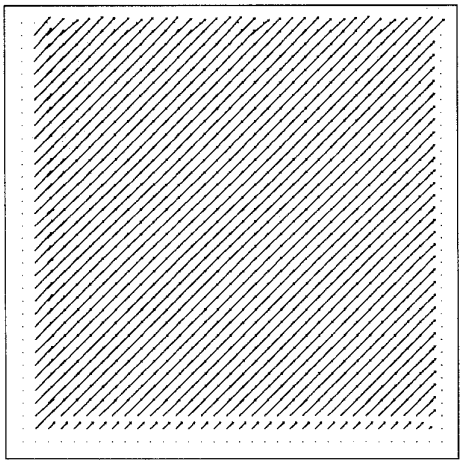

Figure 1: Curve Evolution computed flow field for the sinusoidal synthetic sequence.

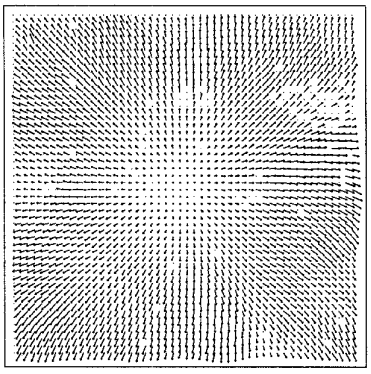

Figure 2: Curve Evolution computed flow field for the diverging tree synthetic sequence.

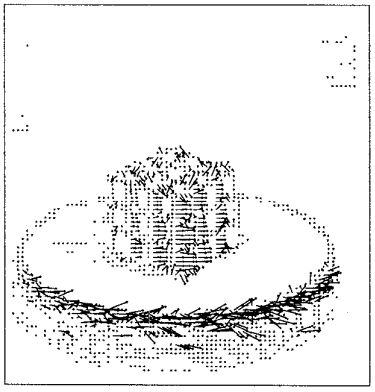

Figure 3: Curve Evolution computed flow field for the rubik's cube sequence.

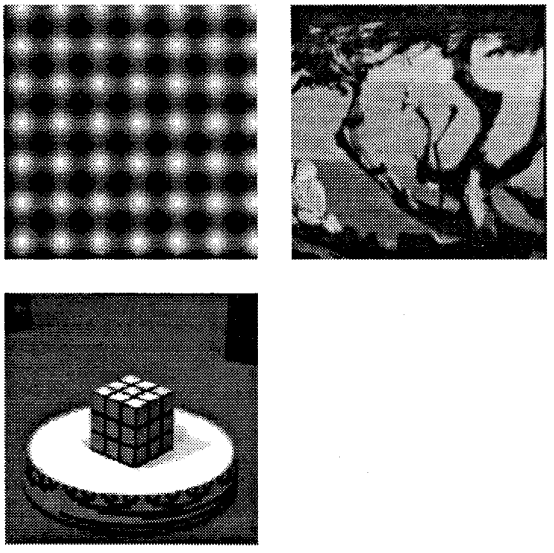

Figure 4: Frames from (a) Sinusoidal (b) Diverging Tree (c) Rubic Cube.